2024 IEEE/RSJ International Conference on Intelligent Robots and Systems (IROS)
October 14-18, 2024. Abu Dhabi, UAE

Development of a Throwbot with Shock Absorption Structure

Jaeyeong Keum, Jaemin Kim, Changgi Lee,
Seunghyun Lim, Insung Ju and Dongwon Yun*, *Senior Member, IEEE*

***Abstract*— In this study, a throwing robot equipped with an shock absorbing structure, utilizing paired-Cross Flexural Hinge (p-CFH) and an airbag, was fabricated and validated to assess the effectiveness of its impact absorption mechanism. This robot was developed in anticipation of situations where direct human intervention for life rescue would be challenging. Throwing robots can be broadly categorized into ball type, wheel type, and hybrid type. The hybrid type combines the advantages of both: the ease of throwing from ball type, due to its low air resistance coefficient, and the versatile mobility of the wheel type in diverse environments. However, hybrid type throwing robots are more vulnerable to external impacts due to the complexity of their internal structure, resulting in a lower maximum drop height compared to wheel type robots.**

To address these challenges, this research proposes a the Throwbot that combines the easy throwing capability of ball type with the obstacle overcoming ability of the wheel type, while also addressing the low free fall height drawback inherent in hybrid types. To achieve this, we developed a Throwbot with a ball to wheel transform structure, p-CFH mechanism, and airbag based impact absorption system. Additionally, materials were selected based on simulation results to refine the Throwbot. The performance of the proposed robot was evaluated through various assessments, including free fall experiments and obstacle overcoming tests. Through this research, the proposed Throwbot effectively addresses the shortcomings of existing throwing robots, establishing a novel approach to throwing robot design.

I. INTRODUCTION

Various types of robots, such as snake robots [1], [2], drones [3], [4], [5], and throwing robots, are being developed to address situations where human access to disaster site is challenging. Among those, throwing robots have the advantage of overcoming obstacles like high walls and passing through narrow areas caused by building debris, making them particularly useful in disaster situations.

Throwing robots can be broadly categorized into ball type, wheel type, and hybrid type. Ball type throwing robots are easy to throw due to their shape, and they have do not tip over. Additionally, the entire surface of the ball type robot provides propulsion, preventing it from being stopped by obstacles on its body, unlike wheel type robots [6]. However, a major disadvantage of ball type robots is their inability to overcome obstacles, limiting them to smooth terrain. In [7], a ball type robot capable of overcoming obstacles is proposed, but its large size and weight of approximately 6.4 kg make it unsuitable for throwing. Conversely, robots specifically designed for throwing, focusing on miniaturization and shock absorption, have been studied, but they lack a movement mechanism [8]. The robot proposed in [9] features a movement mechanism using soft materials, but it is limited by having only one degree of freedom, restricting its various movements. Additionally, the HoYa Robot, introduced in [10] and [11], is a lightweight robot that is easy to throw, but it is vulnerable to shock due to the lack of shock absorption mechanism, with a maximum free fall height of 2 m.

Wheel type throwing robots can operate in various en-

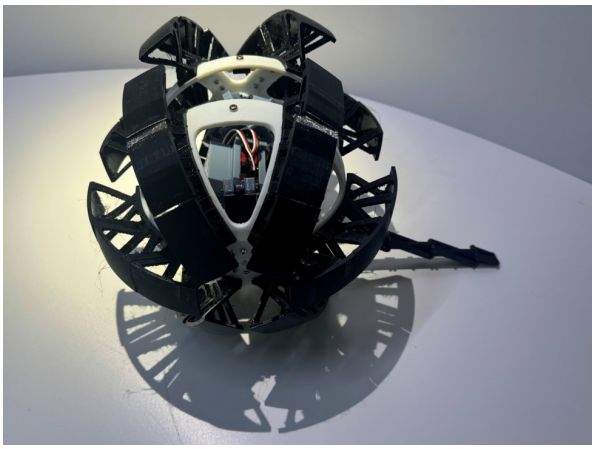

(a)

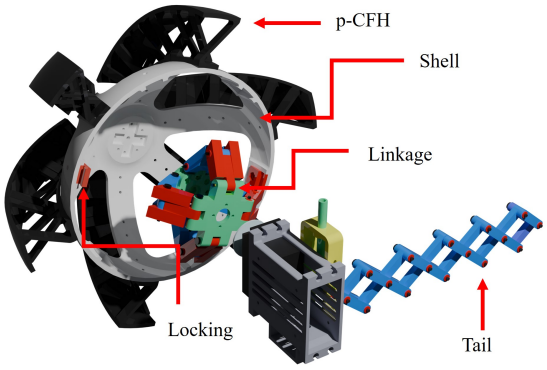

(b)

Fig. 1: (a) Throwbot in wheel mode (b) Exploded view of Throwbot

This work was supported by the Future Defense Innovation Technology Development Project(RS-2023-00284294, "Development of Transformable Throwing Robot with Shock Absorption Structure") funded by National Research Foundation of Korea(NRF). (Corresponding author: Dongwon Yun.)

Authors are with the Department of Robotics and Mechatronics Engineering, Daegu Gyeongbuk Institute of Science and Technology (DGIST), Daegu, 42988 South Korea (e-mail: jykeum@dgist.ac.kr; jaeminkim@dgist.ac.kr; dlckdrl99@dgist.ac.kr; shl0216@dgist.ac.kr; jurobot@dgist.ac.kr; mech@dgist.ac.kr).

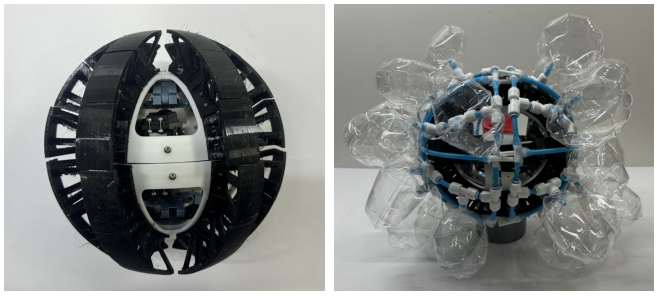

(a) (b)

Fig. 2: (a) Throwbot in ball mode (b) Throwbot with airbag

vironments and have a better ability to overcome obstacles compared to ball type robots. Furthermore, unlike ball type robots, which must maintain a spherical shape for ease of movement and throwing, wheel type robots are not restricted beyond the need for wheel mobility. This allows for the application of various shock absorption mechanisms, such as parachutes [12], flexible hinges [13], aerial attitude control [14], and wheels larger than the robot's body [15]. However, due the shape of wheel type robot, it is sometimes necessary to develop a separate throwing device [16], and additional structures may be required to prevent the body from rotating during movement [17].

Hybrid type throwing robots have a structure that can switch between ball type and wheel type [18], [19]. When the robot lands on the ground, it switches from throwing mode to driving mode to perform its mission. This switchable design allows it to combine the ease of throwing of the ball type with the maneuverability and obstacles overcoming ability of the wheel type. In some cases, a rubberized shell is added to the robot's exterior to absorb shock [20]. However, the cushioning performance of the rubberized shell cannot be improved by reducing hardness or increasing thickness beyond a certain level [20], which limits the throwing height. There are also robots that can transition from a sphere to a three-legged robot [21], as well as those that can change from a tetrahedral structure to a planar structure [22].

In both cases, the additional transformation mechanisms, which are seldom used, increase the robot's weight, making it less suitable for throwing [20]. The main disadvantage of these hybrid structures is their complex internal design, which enables the switch between ball type and wheel type.

To address the disadvantages of these robots, we developed a hybrid type Throwbot (as shown in Fig. 1) that can combine the benefits of the ball type, such as ease of throwing due to its small size, with the obstacle overcoming ability and high speeds of the wheel type. Additionally, to address the reduction in maximum throwing height, we adopted a simplified internal design, including p-CFH and airbag structure, to overcome this limitation. Through this study, we confirmed that p-CFH and airbag structures are effective for throwing robots with shock absorption structures, and we proposed a new method for manufacturing.

II. Design of System

A. System Overview

Throwbot, equipped with shock absorbing structure, incorporates various design techniques to combine the ease of throwing, the obstacle overcoming ability, and addressing the low free fall height limitations of existing throwing robots.

To address the complexity of the internal structure, we designed a ball to wheel transformable simple structure. This design uses a linkage structure that switches from ball mode to wheel mode. To overcome the limitations of ball type throwing robots in absorbing shocks and overcoming obstacle, p-CFH was applied to the exterior shell, allowing the robot to be thrown and operated in various environments. In ball mode, the Throwbot (as shown in Fig. 2a) is equipped with an airbag and is thrown in the configurations shown in Fig. 2b. When the robot hits the ground, the airbag is automatically removed, and it simultaneously switches from ball mode to wheel mode (as shown in Fig. 1a) and begins operation.

Throwbot with a shock absorption structure consists of three main parts. As shown in Fig. 1b, the first is the linkage structure for transforming from ball mode to wheel mode, the second is the tail structure to improve driving stability, and the third is the p-CFH and airbag structure for shock absorption.

The designed throwbot is shown in Fig. 1b. The parts were fabricated using a 3D printer (Bambu Lab X1-Carbon, Bambu Lab, China). The linkage, tail, and shell parts were made using PLA, while the CFH was maded TPU. The driving mechanism consist of a differential drive system with two servo motors (DHV-2288, Sky Holic, South Korea) mounted on a main frame made of PLA. The differential drive system allows the Throwbot to move forward, backward, and rotate in place. The system is powered by a lithium polymer battery (2200 mAh 8c 7.4 V (2S), TOYMIX, South Korea), and a receiver (R7008SB, Futaba, Japan) is used for remote control.

B. Linkages for Transform Ball Mode to Wheel Mode

Throwbot is thrown in ball mode and switches to wheel mode after landing. To solve the issue of reduced throwing height, we simplified the ball to wheel transformable structure. In existing hybrid types, additional actuators are used to switch modes, which complicates the structure, adds weight, and reduces the throwing height. To address this issue, we used a linkage structure and a spring to simplify the design and enable immediate mode changes.

The linkage structure consists of two linkages, one in each shell, with an elongated design measuring, 25 mm when folded and 52 mm when fully extended. The two shells remain folded after the linkage's spring is compressed, secured by the locking structure. When the robot is thrown and impacts the ground, the locking mechanism disengages, allowing the spring to unfold the linkage. If the impact does not disengage the lock, the motor's rotation will do so, ensuring a reliable transformation. If the linkage unfolds

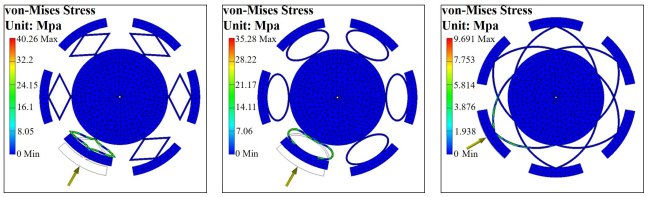

(a) (b) (c)

Fig. 3: Impact absorption simulation of various wheel structures (a) Diamond structure (b) Ellipse structure (c) FH structure

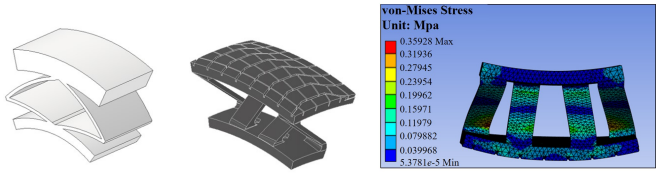

(a) (b) (c)

Fig. 4: Comparison of FH and p-CFH (a) FH structure (b) p-CFH structure (c) Impact absorption simulation of CFH structure

to 180 degrees, additional force is required to revert to ball mode, so the linkage structure is designed to avoid full unfolding. Since the Throwbot only needs to switch to ball mode for throwing, the transformation is only from ball mode to wheel mode, requiring human intervention to reset to ball mode in preparation for the next throwing. This structure is ideal for throwing robots because it does not require additional actuators and is simple, lightweight, and reliable. By adopting this structure, the Throwbot with shock absorbing structure can withstand high impact heights.

C. Tail for Stable Driving

Ball type throwing robots require a tail structure for stable driving and overcoming obstacles [10]. Since the Throwbot is thrown in ball mode, the tail must be stored inside the robot. The tail also needs to be longer than the radius of the robot's outer shell, requiring a variable length structure. To achieve this, we used a mechanism that compresses and stored the tail inside the robot in ball mode, then extend it outside to form the tail when it is thrown and switches to wheel mode.

The tail mechanism is designed with a scissor lift structure. This structure offers the advantage of a compactness and a variable length. Like the previous linkage structure, it was designed to be stored inside the robot in a compressed state without using an actuator, then unlocked and extended by spring force. This design keeps the robot lightweight and compact without the need for additional actuators. The tail, utilizing a scissor lift structure, measures 43 mm when compressed and extends up to 220 mm with a spring, providing a variable length of 177 mm.

III. Design of Shock Absorption Structure

The wheel and airbag structures were desinged through Finite Element Analysis (FEA) before being fabricated based on these predictions.

A. Shock Absorption with p-CFH

To select the most efficient shock absorbing wheel structure, we used Inventor (Autodesk, USA) to design various structures, including diamond, ellipse, Flexural Hinge (FH) structures. These wheel structures were created using nylon with a bending stress of 38.3 MPa, as shown in Fig. 3.

Assuming the robot falls from a height of 6 m with no air resistance and a gravitational acceleration of 9.8 m/s^2, and that the impact is concentrated on one part of the wheel, the velocity at the moment of impact with the ground is approximately $\sqrt{2 \cdot 6 \cdot 9.8} \approx 11$ m/s. Given that the robot weighs 0.8 kg and the shock absorption time is 0.2 s, the resultant force between the robot and the ground is calculated as $11 \cdot 0.8/0.2 = 44$ N. To account for the safety factor, the resultant force used in the FEA using Inventor Stress Analysis (Autodesk, USA) is set to 50 N.

For the diamond structure wheel, as shown in Fig. 3a, a maximum deformation of 6.815 mm and a maximum stress of 40.26 MPa occur, resulting in a safety factor of 0.95, which exceeds the bending stress of nylon and causes the structure to fail. Therefore, the diamond structure wheel is not suitable for shock absorption. For the elliptical structure wheel, as shown in Fig. 3b, a maximum deformation of 4.646 mm and a maximum stress of 35.28 MPa occurs, resulting in a safety factor of 1.08. Although this does not exceed the bending stress of nylon, if a slightly larger force is applied, it will break immediately, therfore the elliptical structure wheel is also not suitable for shock absorption. For the FH structure wheel, as shown in Fig. 3c, a maximum deformation of 0.3424 mm and a maximum stress of 9.691 MPa occurs, resulting in a safety factor of 3.95. This does not exceed the bending stress of nylon, ensuring that the wheel will not break even if a larger force is applied. Therefore, the FH structure was selected for the wheel's shock absorption.

To increase the shock absorption capacity, as shown in Fig. 4, the wheel was designed using TPU, which has a density of 223 kg/m^3 higher than nylon, but offers much higher shock resistance. Additionally, the p-CFH structure, composed of two intersecting independent beams, was applied to the wheel. This design offers excellent shock absorption capacity, unlike the FH structure, which is composed of a single rigid body. The p-CFH structure also resulted in a 20% weight reduction compared to the FH structure.

For a more precise shock absorption analysis, Ansys Static Structural (Ansys, USA) was used to analyze the shock absorption of the p-CFH structural wheel. As in the previous shock absorption simulation, 50 N was set as the FEA input. As shown in Fig. 4c, the simulation result shows a maximum deformation of 2.2332 mm, which is 6.5 times larger than that of the FH structure, but the maximum stress of 0.3593 MPa is 27 times lower. This predicts that the shock absorption capacity of the wheel can be improved using TPU and the p-CFH structure.

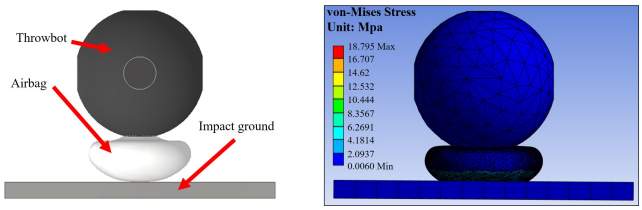

(a) (b)

Fig. 5: Shock absorption simulation of airbag (a) Shock absorption simulation setting (b) Simulation result

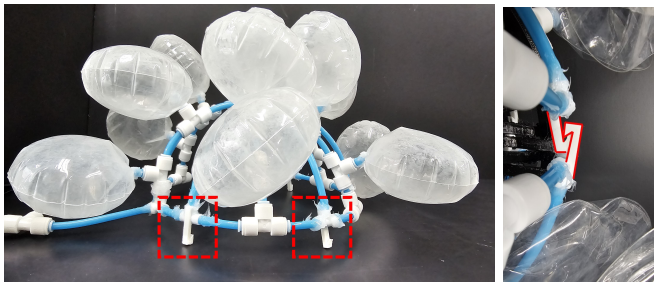

(a) (b)

Fig. 6: Structure of airbag module (a) Single airbag module (b) Locking mechanism for airbag module

B. Shock Absorption with Airbag

To assess the effectiveness of the airbag in absorbing shock when the robot is thrown and collides with the ground, FEM analysis was performed using Ansys Static Structural (Ansys, USA) before actual production. The analysis components included a Throwbot made of PLA, an airbag made of Polyvinyl Chloride (PVC) film, and a structural steel collision surface. The input resultant force was set to 50 N, consistent with the previous wheel structure analysis.

As shown in Fig. 5b, when a force of 50 N was applied to the airbag, the deformation less than 2.7 mm, and the deformation and stress on the robot were almost zero. From this, we can predict that the airbag can effectively absorb the shock from a collision with the ground.

Based on the simulation, an airbag module was created to be mounted on the Throwbot. For the airbag module, we chose a CO_2 cartridge as the gas generator to reuse the airbag. PVC, which is easy to process and durable, was selected to absorb the impact of the airbag, and a durable polyurethane (PU) tube was used to make the flow path.

The airbag module was designed with two hemispheres that wrap around the Throwbot, as shown in Fig. 6a. The coupling with the Throwbot is accomplished by engaging six clasps attached to each hemisphere with corresponding clasps on the opposite side, as shown in Fig. 6b. This structure allows the airbag module to be mounted to the Throwbot without direct coupling. Additionally, when the Throwbot collides with the ground, the airbag module, which is composed of PU tubes, deforms and the fastening structure is distorted, allowing the Throwbot and the airbag module to be separated without any additional device.

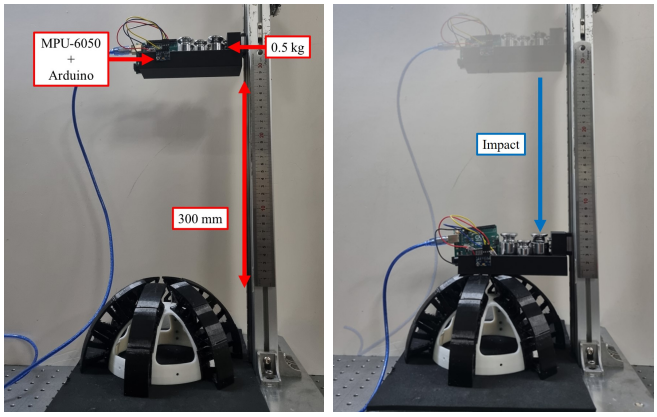

(a) (b)

Fig. 7: Impact absorption experiment setting and process (a) Test setting (b) Impact test process

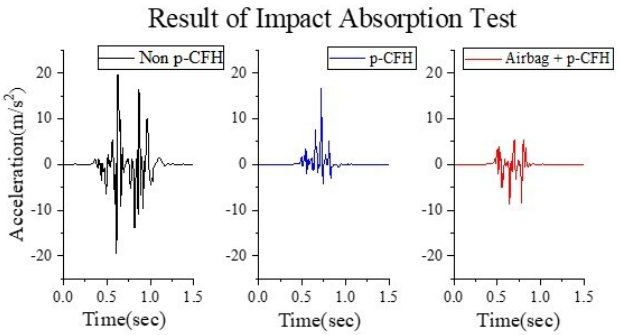

Fig. 8: Acceleration graph of impact absorption experiment

IV. Shock Absorption Structure Experiment

To verify the design of the shock absorption structure, we conducted an experiment to measure the impact by dropping a weight on the shock absorption structure. As shown in Fig. 7, a 0.5 kg weight was dropped from a height of 300 mm onto the structure to measure the resulting acceleration. For the acceleration measurements, the weight was connected to a basket, and we measured the acceleration upon impact by dropping the weight onto three differenet structures: a TPU block without a p-CFH structure, a shell with a p-CFH structure, and a structure combining both airbags and p-CFH. The Head Injury Criterion (HIC) was used to indicate the impact's severity, as measuring acceleration alone does not fully capture the reduction in effect. The HIC can be calculated using the (1) [23], [24].

$$HIC = max\left\{(t_2 - t_1)\cdot\left[\frac{1}{t_2 - t_1}\int_{t_1}^{t_2} a(t)dt\right]^{2.5}\right\} \quad (1)$$

In (1), the interval $t_2 - t_1$ can be up to 36 ms. We conducted the experiment over a total duration of 36 ms [25], centered around the peak value with a range of ± 18 ms.

TABLE I: Peak acceleration and HIC value of experiment

	Acceleration Peak $[m/s^2]$	HIC
Non p-CFH	19.6200	16.3705
Only p-CFH	16.6213	6.3986
Airbag with p-CFH	5.4806	0.3373

As shown in Fig. 8, the p-CFH structure exhibited less acceleration change compared to the block shaped structure, and the acceleration change was further reduced when the airbag was combined with the p-CFH structure. Table I provides a detailed comparison of acceleration and HIC values. The acceleration peak was the lowest at 5.4806 m/s^2 when both the airbag and p-CFH structure were used together, and highest at 19.6200 m/s^2 in the block form with only the p-CFH. When comparing the HIC values, the HIC for the airbag was 0.3373, the p-CFH was 6.3986, and the block was 16.3705, indicating that the combination of the airbag and p-CFH structure effectively reduced the impact. When comparing the reduction in peak value and HIC, the peak value decreased by 15.3%, and the HIC by 60.9% when the p-CFH structure was used, compared to the plain block. The peak value decreased by 67.0%, and the HIC by 94.7% when comparing the results with and without airbags. This confirms that the designed structure effectively reduces the impact on the robot during a fall after a throwing situation.

V. Performance Tests and Result

The developed Throwbot weighs 0.765 kg without the airbag and has a diameter of 220 mm in ball mode. The operating noise of the robot, measured at a distance of 1 m in a quiet indoor environment, was 58.6 dB. Battery life is also a critical factor for this type of robot. To assess this, we operated the robot at its minimum speed and confirmed that it could run for over 75 minutes. In terms of running speed, the robot achieved an average velocity of 0.8257 m/s over a distance of 3 m, repeated five times. The Throwbot is designed with a differential drive robots, and the forward speed is calculated as $V = (v_R + v_l)/2$, where v_R and v_L represent the speeds of the right and left wheels, respectively. By substituting the motor speed and the wheel radius of 0.11 m into the equation, the calculated speed is 1.05 m/s. However, the actual measured speed is lower, which can be attributed to wheel slip and the robot's inability to maintain a straight path, both of which reduce the overall speed. Additionally, since each shell operates as a differential structure, the robot can execute rapid turns and perform various maneuvers, with a rotation speed of approximately 1 rev/s when turning in place.

The shell structure with p-CFH attached to the robot not only contributes to shock absorption but also enhances its ability to overcome obstacles. To verify the robot's ability to overcome obstacles, we conducted experiments on triangular bumps and stairs, as shown in Fig. 9. As a result, the Throwbot successfully overcome a 55 mm step obstacle and a 50 mm high triangular bump.

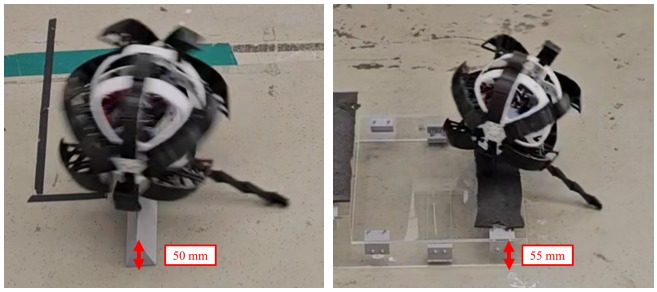

(a) (b)

Fig. 9: Obstacle overcome performance test (a) Triangular bump (50 mm) (b) Step (55 mm)

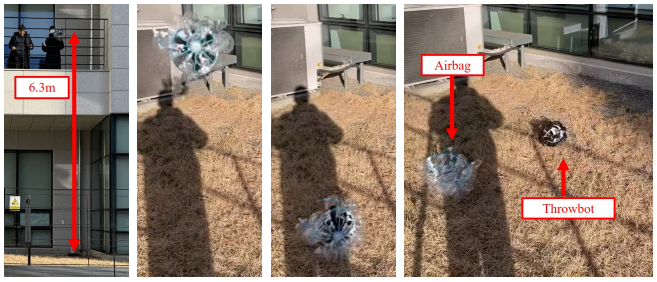

(a) (b) (c) (d)

Fig. 10: Free fall test of Throwbot (a) Experiment setting (b) Free fall (c) Before impact (d) After impact

One of the key performance metrics for a throwing robot is the allowable drop height that does not cause operational issues. To verify the allowable free fall height, the Throwbot was equipped with an airbag and dropped from a height of 6.3 m, as shown in Fig. 10a. Its operational status was then checked to confirm success. After falling from 6.3 m, the Throwbot touches the ground, the airbag automatically detaches from the robot, the shell's locking structure disengages, and the robot transitions to wheel mode. As a result, as shown in Fig. 10, the shock absorption structure of the airbag and p-CFH effectively absorbed the impact, allowing the robot to operate successfully.

Table II compares the performance of the Throwbot with that of existing throwing robots from previous studies. The Throwbot weighs less than 1 kg, making it easy to throw due to its ball type design, and it also showed the fastest running speed among the comparison groups. Additionally, the p-CFH based shock absorption structure and the airbag structure used in the robot allowed for a higher permissible drop height compared to other wheel type robots. Therefore, this confirmed that the proposed robot not only combines the advantages of a ball type robot, which is easy to throw, and a wheel type robot, known for its excellent driving speed and obstacle overcoming performance, but also offers superior shock absorption performance.

VI. Conclusions

The Throwbot, which incorporated the proposed p-CFH and airbag structure to address the limitations of existing

TABLE II: Performance comparison for the throwing reconnaissance robots

Robot	Type	Weight [kg]	Velocity [m/s]	Drop height [m]	Obstacle overcome height [mm]	Size(WLH)[mm]
[13]	Wheel	2.05	0.6	5.6	N/A	217 x 210 x 85
[20]	Hybrid	0.52	0.34	9	N/A	110 (Spherical, Diameter)
[26]	Wheel	0.3	0.45	3 (w/o Camera)	N/A	N/A
[27]	Wheel	10.7	0.33	5	90	355 x 400 x N/A
Ours	Hybrid	0.765	0.8257	6.3	55	220 (Spherical, Diameter)

throwing robots, demonstrated significant improvements in overcoming these shortcomings. Firstly, in terms of overcoming obstacles, experiments confirmed that the p-CFH structure can be used to overcome a 55 mm step obstacle. In addition, the low free fall height caused by the complex internal structures of the wheel type and hybrid type was improved by utilizing a simple linkage structure along with p-CFH and airbags. Notably, p-CFH and airbags were utilized to achieve a free fall height of 6.3 m, a feat difficult to accomplish with existing hybrid type robots. This is due to its low weight, achieved by utilizing an efficient yet simple ball to wheel conversion mechanism and an effective shock absorption structure using p-CFH and airbags. This structure was experimentally validated as effective in a 6.3 m free fall test. This study offers a new direction for the development of throwing robot with shock-absorbing structures using p-CFH and airbags. In the future, we plan to miniaturize and reduce the weight of the shock absorbing structure in the Throwbot to achieve greater free fall heights and improved ease of throwing.

REFERENCES

[1] J. Bae, M. Kim, B. Song, J. Yang, D. Kim, M. Jin, and D. Yun, "Review of the latest research on snake robots focusing on the structure, motion and control method," *International Journal of Control, Automation and Systems*, vol. 20, no. 10, pp. 3393–3409, 2022.

[2] J. Bae, M. Kim, B. Song, M. Jin, and D. Yun, "Snake robot with driving assistant mechanism," *Applied Sciences*, vol. 10, no. 21, p. 7478, 2020.

[3] S. M. S. M. Daud, M. Y. P. M. Yusof, C. C. Heo, L. S. Khoo, M. K. C. Singh, M. S. Mahmood, and H. Nawawi, "Applications of drone in disaster management: A scoping review," *Science & Justice*, vol. 62, no. 1, pp. 30–42, 2022.

[4] A. Restas, "Drone applications for supporting disaster management," *World Journal of Engineering and Technology*, vol. 3, no. 3, pp. 316–321, 2015.

[5] B. Mishra, D. Garg, P. Narang, and V. Mishra, "Drone-surveillance for search and rescue in natural disaster," *Computer Communications*, vol. 156, pp. 1–10, 2020.

[6] S. B. Pandey, M. D. Rawat, H. B. Rathod, and J. M. Chauhan, "Security throwbot," in *2017 International Conference on Inventive Systems and Control (ICISC)*. IEEE, 2017, pp. 1–6.

[7] T. J. Ylikorpi, A. J. Halme, and P. J. Forsman, "Dynamic modeling and obstacle-crossing capability of flexible pendulum-driven ball-shaped robots," *Robotics and Autonomous Systems*, vol. 87, pp. 269–280, 2017.

[8] J. Pfeil, K. Hildebrand, C. Gremzow, B. Bickel, and M. Alexa, "Throwable panoramic ball camera," in *SIGGRAPH Asia 2011 Emerging Technologies*, 2011, pp. 1–1.

[9] Y. Masuda and M. Ishikawa, "Development of a deformation-driven rolling robot with a soft outer shell," in *2017 IEEE International Conference on Advanced Intelligent Mechatronics (AIM)*. IEEE, 2017, pp. 1651–1656.

[10] W. Jung, Y. Kim, and S. Kim, "Design of a miniature sphere type throwing robot with an axial direction shock absorption mechanism," *Journal of Institute of Control, Robotics and Systems*, vol. 21, no. 4, pp. 361–366, 2015.

[11] K. Kim and J. Kim, "A research of the development plan for a highly adaptable fsr (fire safety robot) in the scene of the fire," *Fire Science and Engineering*, vol. 24, no. 3, pp. 113–118, 2010.

[12] T. Shimizu, S. Hayashi, T. Midorikawa, T. Fujikawa, E. Takane, M. Watanabe, K. Tadakuma, M. Konyo, and S. Tadokoro, "Small swarm search robot system with rigid-bone parachute rapidly deployable from aerial vehicles," in *2019 IEEE International Symposium on Safety, Security, and Rescue Robotics (SSRR)*, 2019, pp. 88–93.

[13] W. Wang, S. Wu, P. Zhu, and X. Li, "Design and experimental study of a new thrown robot based on flexible structure," *Industrial Robot: An International Journal*, vol. 42, no. 5, pp. 441–449, 2015.

[14] D. J. Gonzalez, M. C. Lesak, A. H. Rodriguez, J. A. Cymerman, and C. M. Korpela, "Dynamics and aerial attitude control for rapid emergency deployment of the agile ground robot agro," in *2020 IEEE/RSJ International Conference on Intelligent Robots and Systems (IROS)*, 2020, pp. 2577–2584.

[15] D. O'Halloran, A. Wolf, and H. Choset, "Design of a high-impact survivable robot," *Mechanism and machine theory*, vol. 40, no. 12, pp. 1345–1366, 2005.

[16] H. Lu, J. Gao, J. Zhao, Y. Liu, X. Li, Z. Xu, H. Cao, F. Zhao, X. Shi, and L. Wang, "Mechanical design of aerial dispersal miniature reconnaissance robot launch module," in *2015 IEEE International Conference on Information and Automation*, 2015, pp. 83–88.

[17] D. Lee, G. Jung, M. Sin, S. Ahn, and K. Cho, "Deformable wheel robot based on origami structure," in *2013 IEEE International Conference on Robotics and Automation*, 2013, pp. 5612–5617.

[18] C. Ye, G. Ma, and S. Ma, "Development of a throwable shape-shifting spherical robot," in *2014 IEEE International Conference on Mechatronics and Automation*. IEEE, 2014, pp. 641–645.

[19] T. Mathew, G. Knox, W. Fong, T. Booysen, and S. Marais, "The design of a rugged, low-cost, man-packable urban search and rescue robotic system," in *Proceedings of the robotics and mechatronics conference of South Africa, Cape Town, South Africa*, 2014, pp. 27–28.

[20] R. Liu and Y. Qu, "Transformation design of a miniature throw-able robot," *Industrial Robot: An International Journal*, vol. 41, no. 2, pp. 145–156, 2014.

[21] P. Jearanaisilawong, S. Laksanacharoen, V. Piriyawong, and K. Swatdipisal, "Design of a three-legged reconfigurable spherical shape robot," in *2009 IEEE/ASME International Conference on Advanced Intelligent Mechatronics*, 2009, pp. 1730–1733.

[22] K. Tadakuma, R. Tadakuma, K. Nagatani, K. Yoshida, M. Aigo, M. Shimojo, and K. Iagnemma, "Throwable tetrahedral robot with transformation capability," in *2009 IEEE/RSJ International Conference on Intelligent Robots and Systems*, 2009, pp. 2801–2808.

[23] J. Yang, J. Kim, D. Kim, and D. Yun, "Shock resistive flexure-based anthropomorphic hand with enhanced payload," *Soft Robotics*, vol. 9, no. 2, pp. 266–279, 2022.

[24] J. Versace, "A review of the severity index," 1971.

[25] B. G. McHenry, "Head injury criterion and the atb," *ATB Users' group*, vol. 29, pp. 5–8, 2004.

[26] A. Parness and C. McKenzie, "Drop: The durable reconnaissance and observation platform," *Industrial Robot: An International Journal*, vol. 40, no. 3, p. 218–223, Apr 2013.

[27] F. Zhao, J. Gao, J. Zhao, Y. Liu, H. Cao, X. Shi, and C. Liu, "Remote-launch six-wheeled miniature reconnaissance robot," *Mechatronics and Automation Engineering*, Jan 2017.